

Effect of Water Migration between Arabinoxylans and Gluten on Baking Quality of Whole Wheat Bread Detected by Magnetic Resonance Imaging (MRI)

Juan Li,[†] Ji Kang,[†] Li Wang,[†] Zhen Li,[†] Ren Wang,[†] Zheng Xing Chen,^{*,†} and Gary G. Hou^{*,§}

[†]School of Food Science and Technology, State Key Laboratory of Food Science and Technology, Jiangnan University, Wuxi, Jiangsu 214122, People's Republic of China

[§]Wheat Marketing Center, 1200 N.W. Naito Parkway, Suite 230, Portland, Oregon 97209, United States

ABSTRACT: A new method, a magnetic resonance imaging (MRI) technique characterized by T_2 relaxation time, was developed to study the water migration mechanism between arabinoxylan (AX) gels and gluten matrix in a whole wheat dough (WWD) system prepared from whole wheat flour (WWF) of different particle sizes. The water sequestration of AX gels in wheat bran was verified by the bran fortification test. The evaluations of baking quality of whole wheat bread (WWB) made from WWF with different particle sizes were performed by using SEM, FT-IR, and RP-HPLC techniques. Results showed that the WWB made from WWF of average particle size of 96.99 μm had better baking quality than those of the breads made from WWF of two other particle sizes, 50.21 and 235.40 μm . T_2 relaxation time testing indicated that the decreased particle size of WWF increased the water absorption of AX gels, which led to water migration from the gluten network to the AX gels and resulted in inferior baking quality of WWB.

KEYWORDS: magnetic resonance imaging (MRI), arabinoxylan (AX), gluten, water migration, whole wheat bread

INTRODUCTION

Whole wheat bread (WWB) is one of the fastest-growing staple foods in Western countries.¹ Many scientific studies have confirmed its antioxidative activity and other nutritional functions in epidemiology.^{2–5} However, due to the less cohesive (also water partitioning during mixing and baking) property of whole wheat dough (WWD) compared with that of white dough, the baking qualities of WWB, including loaf volume, specific volume, and interior structure (the porosity of bread), are inferior to those of white bread,⁶ which has restricted a wider acceptance of WWB by consumers.⁷ In Asian countries, there are many fewer whole wheat products and a lower market shares, leading to increased incidence rates of chronic diseases and reduced value of grains (more grain components go to feed).⁸

The relationship between the particle size of wheat bran and the volume of bread has been investigated, but the results were inconclusive and controversial. Some studies have shown that the wheat bran has a negative effect on bread volume,^{9,10} especially small bran particles.^{11,12} Wheat bran particles can deleteriously affect the gluten network, decrease dough resilience, and impair the framework of gas cells and, thus, gas retention. These effects can lead to low bread specific volume and inferior baking quality.¹³ However, other research has shown that bread made from smaller bran particle size flour had a larger volume than bread made with coarser bran flour.¹⁴ Meanwhile, there were some results suggesting that bread with the medium particle size (415 μm) of wheat bran had larger volume than either the refined (278 μm) or the coarse group (609 μm).⁹ More studies are still needed to investigate the effect of whole wheat flour (WWF) particle size on its baking quality.

Arabinoxylans (AX) are important nonstarch polysaccharides that form the cell walls of cereal endosperm and bran.¹⁵ Ferulic acid (FA) is a major phenolic acid in wheat, where it is mainly esterified to the arabinose backbone of AX.^{16,17} In wheat bran, it is concentrated in cell walls. Incorporation of ferulic acid into arabinose residues enhances the formation of intermolecular cross-links of AX, leading to gel formation.¹⁸ Previous research reported that the AX gels can inhibit the formation of gluten network by changing water distribution among gluten and other macromolecules and result in a less extensible gluten.¹⁹ This is especially true when AX gels compete with the gluten network for water during mixing, restraining the gluten network from water uptake.²⁰ Gill²¹ proposed the redistribution of water from nonstarch polysaccharides to gluten during fermentation. Jacobs⁷ theorized that AX tightly binds water in the dough system, reducing the availability of water for developing the gluten network. Roman-Gutierrez et al.²² compared the water vapor adsorption properties of wheat flour and flour components (pentosans, gluten, and starch) using a controlled atmosphere microbalance, and the theoretical distribution of water between the flour components was determined under a water vapor environment. Roman-Gutierrez et al. demonstrated that the water vapor adsorption properties of wheat flour depended only on the ability of the flour components to interact directly with the water molecules, which may not apply to the bread dough system that traps a large amount of water

Received: March 19, 2012

Revised: June 13, 2012

Accepted: June 15, 2012

76 inside macromolecular complexes formed by the swollen
77 components.

78 The magnetic resonance imaging (MRI) technique is a tool
79 for the noninvasive determination of moisture distribution in
80 high-moisture samples, including grain kernels.²³ Traditionally,
81 MRI was applied to examine macro-water distribution and
82 migration in grain, such as water migration in single rice kernels
83 during the tempering process,²⁴ water penetration into rice
84 grains during soaking,²⁵ and water redistribution in grain
85 kernels during drying.²⁶ Moreover, MRI techniques have been
86 developed to show the internal structure of bread, which can
87 simplify the complicated and time-consuming process of
88 sensory and visual instrumental evaluation and reduce
89 costs.^{27,28} MRI has been considered to be an accurate and
90 nondestructive method for visualizing the internal network
91 structure of bread²⁹ and calculating the porosity of air
92 cells.^{30–32}

93 The present work was undertaken to evaluate the effect of
94 WWF particle size on bread-baking performances that were
95 characterized by loaf volume and crumb porosity. To gain more
96 insight into relationships between particle size and bread
97 quality, a MRI technique was applied to examine the water
98 migration between macromolecules (AX gels and gluten). To
99 the best of our knowledge, despite the plenitude of hypotheses
100 that have been proposed concerning water migration and
101 competitive water absorption between AX gels and the gluten
102 network, no definitive evidence has been presented to support
103 these mechanisms. The present study's goal was to verify the
104 water migration pattern and competitive water absorption
105 mechanism between AX gels and gluten through the MRI
106 technique and to confirm that it was the mechanism of inferior
107 loaf volume of WWB caused by refined particle size flour.

108 ■ MATERIALS AND METHODS

109 **Wheat Grain.** Wheat grain (Zheng 9023 cultivar, harvested in
110 2008) was obtained from Jin Lenong Agriculture Development Co.,
111 Ltd. (Henan Province, China).

112 **WWF Analysis.** Ash content (12% moisture basis) was 1.60% and
113 protein content (12% moisture basis, N × 5.7) was 13.0%, as reported
114 by the supplier. Farinograph curves were obtained according to AACC
115 International Approved Method 54-21.

116 **Chemicals.** Bakery sugar, salt, shortening, and instant dry yeast
117 were purchased from a local supermarket. The chemicals used for
118 preparing scanning electron microscopy (SEM) samples and testing
119 the content of FA were of analytical grade and purchased from
120 Sinopharm Chemical Reagent Co. (Shanghai, China).

121 **WWF Milling.** The WWF was milled from intact wheat kernel
122 samples using a Waring blender (DFY-400, Wenling Dade Traditional
123 Chinese Medicine Machinery Co., Ltd., Zhejiang Province, China) by
124 grinding for 5 min. The coarse flour was superfine ground by the
125 ultramicro pulverizer (MZP-4, Hengtai Dongqi Powder and Equip-
126 ment Co., Ltd., China) for 15, 25, and 35 min, respectively to achieve
127 the desired particle sizes. Four hundred grams WWF of each particle
128 size group was prepared each time. All experiments were repeated
129 three times.

130 **Particle Size Analysis.** The particle size distributions of WWF
131 obtained from different milling times were measured by the Laser
132 Particle Size Analyzer (S3500, Microtrac Inc., USA), and the
133 measurements were triplicates. The data were fitted by Origin
134 (version 8.5), and the average particle size was obtained from the
135 fitted curve.

136 **Breadmaking.** Bread loaves (each made from 150 g of dough)
137 were made in duplicate using AACC Approved Method 10-10B
138 (optimized straight-dough; AACC International, 2000) with some
139 adjustments. Formulation was as follows: WWF, 500 g; sugar, 30 g;
140 salt, 7.5 g; shortening, 15 g; and instant dry yeast, 15 g. Control bread

was prepared from a commercial white bread flour (China Oil and
141 Foodstuffs Corp., Qinhuangdao, Hebei, China). Commercial bread
142 flour quality parameters were as follows: ash content, 0.40% (14% mb)
143 and protein content, 14.0% (14% mb). Yeast was dissolved in water
144 containing 0.1% sugar at 30 °C before use. Optimum absorption of
145 68% was acquired from the Farinogram data (11.3% mb). Dough was
146 mixed in a bread mixer (hook-mixer with a 1 kg mixing bowl;
147 Guangzhou Chenggong Baking Machinery Co., Ltd. China).
148 Ingredients were mixed at speed 2 for 5–8 min (optimized in
149 preliminary assays). Then the dough was divided into 150 g per piece,
150 placed into a rectangular baking pan (10 × 5 × 3 cm), and fermented
151 at 27 °C for 30 min, which was adjusted from the 90 min adopted in
152 AACC International Approved Method 10-10B (2000) to avoid dough
153 collapse after a long fermentation time. Then, the dough was punched
154 down and proofed for 90 min (increased from 33 min, because this
155 was found to greatly improve the volume of WWB) at 38 °C with 85%
156 relative humidity in a proofing cabinet. Baking was conducted in an
157 oven (HXM-CS11-10, Shanghai Qingyou Industrial Co., Ltd., China)
158 for 25 min at 170 °C upper temperature and 210 °C bottom
159 temperature. After cooling for 1 h, bread samples were placed into
160 plastic bags and stored in a freezer at –18 °C until analyses. Bread
161 slices (1.0 cm) were cut by an electronic bread cutter for MRI analysis.

Evaluation of Bread Quality. Determination of Bread Specific
163 **Volume.** After cooling for 1 h at room temperature on metal grids, the
164 bread weight and volume were measured in triplicates. Bread volume
165 was determined by the rapeseed displacement method (AACC
166 International Approved Method 10-05). The specific volume (cm³
167 g⁻¹) of bread was calculated by dividing the volume by the weight.

Calculation of the Bread Porosity from MR Images. The crumb
169 structure of the WWB slices was evaluated for porosity, as observed
170 with an MRI system (Mini MR-60, Shanghai Niumag Electronics
171 Technology Co., Ltd., Shanghai, China). Image analysis was performed
172 by the spin-echo 2D-FT method using an echo time of 0.1 ms and a
173 repetition time of 0.5 s according to the testing parameters provided
174 by the instrument manufacturer (Shanghai Niumag Electronics
175 Technology Co. Ltd.). The images were recreated on a 192 × 192
176 matrix for 2D images, which were scanned for three layers with a 4.9
177 mm thickness of each layer. The porosity was calculated by the image
178 twice-threshold segmentation method³³ using Matlab (version
179 R2010a) to offset the variation error caused by the signal-to-noise
180 ratio of the scanned images. The gray value range of image was 0–255.
181 The contrast of the images was adjusted and selected from the gray
182 value for detecting the rim of the bread sample; the pixel amount of
183 bread sample was designated N_1 . The threshold value was adjusted and
184 selected again for testing the internal gas cell of the bread; the pixels
185 lower than the threshold were counted and designated N_2 ,
186 representing the gas cells of the bread crumb. Therefore, the pixels
187 that were higher than the threshold represented the backbone
188 structure of the bread. The porosity can be calculated from eq 1
189 provided by the instrument manufacturer (Shanghai Niumag
190 Electronics Technology Co. Ltd.). N is the number of pixels, S_{pixel} is
191 the physical area of a single pixel, and h is the thickness of a bread
192 cross section. V_{pore} is the total volume of the gas cells, and V_{total} is the
193 total volume of the bread, including the gas cell volume and the
194 volume of bread crumb.
195

$$\phi_{\text{MRI}} = \frac{V_{\text{pore}}}{V_{\text{total}}} \times 100\% = \frac{N_2 S_{\text{pixel}} h}{N_1 S_{\text{pixel}} h} \times 100\% = \frac{N_2}{N_1} \times 100\% \quad (1)$$

Evaluation of Effect of WWF Particle Size on Bread-Baking
196 **Quality. SEM.** The interaction between the wheat bran and gluten
197 matrix was observed by scanning electron microscope (Quanta-200,
198 FEI Co., Ltd., USA). The WWB (dough samples were taken after they
199 were properly mixed during the bread-baking process) was fixed with
200 aqueous 3.0% (v/v) glutaraldehyde for 72 h and washed six times with
201 0.1 M sodium phosphate buffer (pH 7.2) followed by aqueous 1.0%
202 (w/v) OsO₄ for 2 h at 4 °C. Samples were then rinsed for 1 h in
203 distilled water and dehydrated in a graded acetone series in five steps.
204 After drying with a critical point dryer, the samples were mounted on 205

206 bronze stubs and sputter-coated with gold (50 Å thick). Then
207 specimens were observed and photographed with an accelerating
208 voltage of 5.0 kV and viewed at magnification levels of 1200X.

209 **Fourier Transform Infrared Spectroscopy (FT-IR).** Three doughs
210 (100 g/each) were produced by mixing three different particle sizes of
211 WWF with 68% D₂O (w/w) (for deducting the background of the
212 pure water) for 3 min using the same bread mixer as described
213 previously. The secondary structure of gluten protein in WWF was
214 determined in triplicates by FT-IR (NEXUS, Nicolet Co., Ltd., USA).
215 The data were processed by Omnic and Peak Fit software (version
216 4.1.2).³⁴

217 **Determination of FA Content by Reversed Phase High-**
218 **Performance Liquid Chromatography (RP-HPLC).** *Extraction of*
219 *FA from WWF.* WWF (2 g) and distilled water (11.3 g) were weighed
220 into a 250 mL shake flask, and the mass fraction of WWF was 15% (w/
221 w). Thermostable α-amylase (0.002 g; 30 U/mg, Novozyme,
222 Denmark) was added. The starch component in WWF was hydrolyzed
223 in ab 84 °C thermostatic water bath for 40 min. The α-amylase was
224 inactivated in a 100 °C boiling water bath for 10 min. After the
225 samples were hydrolyzed, alkali protease (0.001 g, 100 U/mg,
226 Novozyme) was added to the solution, the pH value was adjusted
227 to 8.0 with sodium hydroxide (1.5% w/v), and the mixture was shaken
228 in a water bath (55 °C) for 120 min. After hydrolysis by alkali
229 protease, the enzyme was inactivated by a 100 °C boiling water bath
230 for 10 min. Glucoamylase (0.5 mg; 100 U/mg, Novozyme) was added,
231 and the pH of the solution was adjusted to 4.5 with 2 mol/L
232 hydrochloric acid. The samples were shaken in a water bath (60 °C)
233 for 120 min, after which the glucoamylase was inactivated in a boiling
234 water bath for 10 min. The suspension was centrifuged at 4 °C for 15
235 min at 5000 rpm, and the residue was decanted into another 250 mL
236 shake flask. Finally, 150 mL of sodium hydroxide (1.5% w/v) was
237 added for alkali hydrolyzation in a water bath (85 °C) for 2 h. The
238 suspension was centrifuged for 15 min at 8000 rpm. The pH of the
239 supernatant (5 mL) was adjusted to 2.5 with 2 mol/L hydrochloric
240 acid. The FA was extracted by 10 mL of diethyl ether for 5 min, and
241 the diethyl ether was evaporated using a rotary evaporator (RV 10
242 basic, IKA, Germany) at 45 °C. The FA extract was dissolved by 2 mL
243 of methanol. All of the experiments were conducted in three replicates.
244 **RP-HPLC Analysis of FA.** The FA extract was identified and
245 quantified in triplicate by RP-HPLC (Agilent Technologies, Palo Alto,
246 CA, USA) with UV-diode array absorption. The samples were eluted
247 using a Lichrosphere C-18 (2.1 × 250 mm) column at 30 °C. The
248 mobile phase was 70:30 (v/v) acetonitrile/water with 0.05%
249 trifluoroacetic acid (TFA). The flow rate was 0.8 mL/min, and the
250 detection wavelength was 320 nm. The concentration of FA standard
251 (HPLC ≥ 98%; supplied by Shanghai Yuanye Biotechnology Co., Ltd.,
252 Shanghai, China) was 1 mg/mL, and the injection volume was 1 μL.
253 All solvents were of HPLC grade and filtered through a 0.45 μm
254 membrane. The FA content of samples was calculated from the peak
255 area.³⁵

256 **Determination of T₂ Relaxation Time by NMR.** The relaxation
257 measurements were performed on a Niumag Desktop Pulsed NMR
258 Analyzer (Shanghai Niumag Electronics Technology Co. Ltd.) with a
259 magnetic field strength of 0.54 T and a corresponding resonance
260 frequency for protons of 23.01 MHz. The NMR instrument was
261 equipped with a 60 mm probe. Transverse relaxation (T₂) was
262 measured using the Carr–Purcell–Meiboom–Gill (CPMG) pulse
263 sequence, with a τ value (time between the 90° and 180° pulses) of 75
264 μs. Data from 2000 echoes were acquired as eight-scanned repetitions.
265 The repetition time between two successive scans was 2 s. All
266 relaxation measurements were performed at 25 °C. The T₂ relaxation
267 time was analyzed by the distributed exponential fitting analysis using
268 the Multi Exp Inv Analysis Software developed by Niumag Co., Ltd.,
269 China. A continuous exponentials distribution of the CPMG
270 experiment was defined by eq 2

$$g_i = \int_0^{\infty} A(T) e^{-\tau_i/T} dT \quad (2)$$

271 where g_i is the intensity of the decay at time τ_i and A(T) is the
272 amplitude of the component with transverse relaxation time T.

Equation 2 was solved using Multi Exp Inv Analysis software by 273
minimizing the function 3 274

$$\left(g_i - \int_{x=1}^m f_x e^{-\tau_i/T_x} dT \right)^2 + \lambda \sum_{x=1}^m f_x^2 \quad (3)$$

In formula 3, λ is the weighting and λ∑_{x=1}^m f_x² is a linear combination of 275
functions added to the equation to perform a zero-order 276
regularization.³⁶ The data were pruned from 2000 to 200 points 277
using sampling pruning. This analysis resulted in a plot of relaxation 278
amplitude for individual relaxation processes versus relaxation time. 279
The time constant for each peak was calculated from the peak position, 280
and the corresponding water contents were determined by cumulative 281
integration. All calculations were measured using an in-house program 282
written in combination of Matlab (Mathworks Inc., Natick, MA, USA) 283
and Delphi (Borland, USA). 284

Three grams of bread dough prepared as described under 285
Breadmaking was taken and placed into a test tube immediately 286
after mixing. The water migration between AX gels and gluten in 287
WWD systems with different particle size flours was observed using 288
the NMR system that is represented by spin–spin relaxation times 289
(T₂). 290

RESULTS AND DISCUSSION 291

Effects of WWF Granulation on Bread Volume and 292
Specific Volume. Generally, flour particle size that was 293
measured by the laser particle size analyzer was a multipeak 294
distribution. To obtain the average particle size of flour, the 295
normal multipeak data were further processed with Origin 296
software to fit a Gaussian distribution curve. The average 297
particle sizes of the flour were the peak values of the fitted 298
curves (Figure 1). The average particle sizes of three types of 299 fl

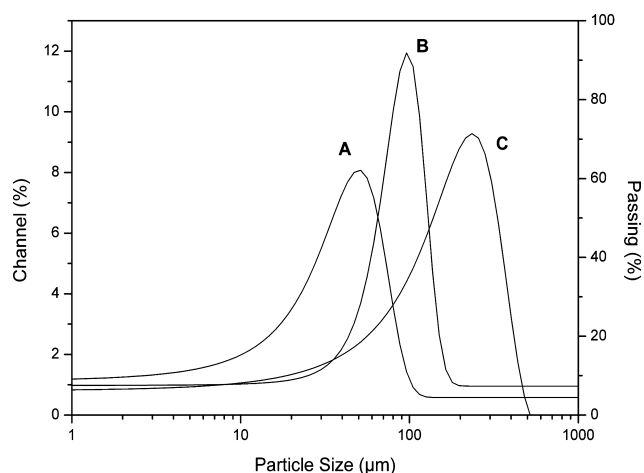


Figure 1. Fitted particle size distribution curves of whole wheat flour (WWF): (A) WWF with an average particle size of 50.21 μm, which was superfine ground by the ultramicro pulverizer for 15 min; (B) superfine ground for 25 min, average particle size of 96.99 μm; (C) superfine ground for 35 min, average particle size of 235.40 μm. The average particle size of the control flour (commercial flour) was 91.20 μm.

WWF from the milling experiment were 50.21 μm (A), 96.99 300
μm (B), and 235.40 μm (C), respectively. The average particle 301
size of commercial bread flour (control) was 91.20 μm. 302

In the baking experiment, the effect of WWF of different 303
particle sizes on baking quality was investigated. The results 304
showed that the volume and specific volume of bread from 305
WWF were lower than those of the white bread (Table 1). In 306
addition, the WWB made from a medium particle size (96.99 307

308 μm) WWF had larger volume and specific volume than those of
309 the coarse (235.40 μm) or refined groups (50.21 μm).

Table 1. Volume and Specific Volume of Whole Wheat Bread Baked from Whole Wheat Flour of Different Particle Sizes^a

particle size (μm)	volume (cm^3)	weight (g)	specific volume (cm^3/g)
control ^b	311.7 \pm 16.1 a	61.2 \pm 1.8 a	5.1 \pm 0.2 a
50.21	193.3 \pm 7.6 c	57.1 \pm 0.8 c	3.4 \pm 0.2 c
96.99	250.0 \pm 13.2 b	59.2 \pm 0.6 b	4.2 \pm 0.2 b
235.40	223.3 \pm 5.8 b	59.7 \pm 2.0 b	3.7 \pm 0.1 b

^aData are the mean value \pm standard deviation. Values in the same column with the same letters are not significantly different ($P < 0.05$).

^bThe control groups were made with commercial white flour. The average particle size of the control flour was 91.20 μm .

310 **Effect of WWF Granulation on the Porosity of WWB.**
311 Three-layer scanned images (Figure 2) of WWB cross sections

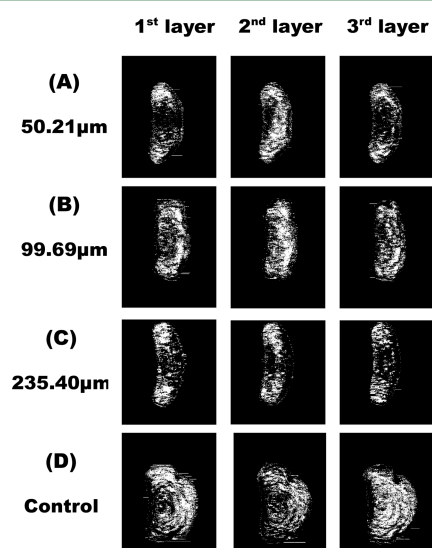


Figure 2. Weighted density of proton images scanned for three layers by the MRI system and processed using the threshold segmentation method: (A, B, C, D) scanned images of longitudinal sections of bread baked from whole wheat flour of particle sizes of 50.21, 96.99, 235.40, and 91.20 μm (control), respectively. The bright area of the scanned images is gas cells, and the dark part represents the bread skeleton.

312 were examined by the MRI system. The breads were baked
313 from WWF of particle sizes of 50.21 μm (Figure 2A), 96.99 μm
314 (Figure 2B), 235.40 μm (Figure 2C), and the control group
315 (made from the commercial white flour) (Figure 2D),
316 respectively. The bright areas of the images were gas cells,
317 whereas the dark parts were bread skeleton. The greatest
318 number and best distribution of gas cells were observed in the
319 control group (Figure 2D) due to noninterference of wheat
320 bran in the structure of the gluten network. Figure 2B shows
321 more gas cells and better gas cell distribution than Figure 2A,C,
322 especially on the second scanned layer, but slightly fewer than
323 the control group. Although the differences of bright area
324 between panels A and C of Figure 2 were not significant, the
325 distribution of gas cells can still be observed. Also, the
326 calculation of porosity can give secondary proof of the
327 differences more precisely. The porosity (Table 2) calculated

by the twice-threshold segmentation method also showed a 328
similar trend. The breads made with WWF of particle size of 329
96.99 μm had a better crumb structure and baking performance 330
than the other two WWF with larger or smaller bran particle 331
sizes, but was second to the control group. The large particle 332
wheat bran in WWF (235.40 μm) caused shearing and diluted 333
the gluten matrix, inhibiting the formation of the gluten 334
network and the structure and integrity of gas cells, which led 335
to reduced gas retention by gluten protein membrane.³⁷ Thus, 336
an uneven distribution of gas cells was formed during the 337
releasing process of CO_2 gas in the early stage of baking. Small 338
particles of wheat bran had a less destructive effect on the 339
formation of the gluten network. However, Figure 2C also 340
shows that the WWB with the smallest bran particle size had 341
less porosity than the medium bran size group. To explain this 342
phenomenon, we tentatively proposed that the dispersion of 343
certain active compounds increased with the refinement of 344
WWF particle size, especially the FA (a component of the AX 345
gels), which has the ability to strengthen the AX gels.³⁸ Due to 346
the better water sequestering capability of the AX gels than of 347
the gluten matrix, the AX gels competed for water with the 348
gluten network in WWB.²⁰ Thus, the formation of gluten was 349
inhibited, because sufficient water for adequate protein 350
hydration is a prerequisite for the development of gluten 351
network. The quality of the gluten network determines the 352
baking performance, so the fine particle size WWF (50.21 μm) 353
led to less porosity than the medium particle size groups. 354

The competitive water sequestering between the AX gels and 355
gluten network in the dough system was confirmed by the 356
measurement of T_2 relaxation time using the MRI technique as 357
detailed under Determination of T2 Relaxation Time by NMR. 358

Effect of WWF Granulation on the Gluten Network. 359
Wheat bran can dilute and disrupt the gluten network, impair 360
gas retention and bread texture and appearance,⁷ and decrease 361
the degree of softening and loaf volume.³⁹ Figure 3 shows 362
various effects on the gluten network by wheat bran of various 363
particle sizes: 50.21 μm (A), 96.99 μm (B), 235.40 μm (C), 364
and 91.20 μm (control, D), respectively. In Figure 3A, a 365
continuous and compact gluten network was observed resulting 366
from the small particle size of the wheat bran. The continuous 367
gluten matrix provided the precondition for superior baking 368
quality, but an excessively compact gluten matrix was 369
detrimental in obtaining good loaf volume.⁴⁰ In Figure 3B, 370
the particle size of the bran was increased (indicated by the 371
arrow), the shearing effect on the gluten matrix was increased, 372
and the gas retention ability was weakened. In Figure 3C, the 373
large particle size of wheat bran (indicated by the arrow) was 374
present in the dough system; it sheared the gluten matrix 375
significantly. The internal structure of the gluten network was 376
fractured, discontinuous, and full of "clutter holes". During the 377
fermentation and proofing stages of the baking process, the gas 378
cells expand into an open network of pores.⁴¹ The fragmented 379
gluten network was unable to retain the CO_2 gas, and the gas 380
was released in the early stages of breadmaking,⁴² leading to 381
small bread volume and inferior baking results. 382

Effect of WWF Granulation on the Secondary 383
Structures of Gluten Protein. Seyer and Gelinas proposed 384
that the deleterious effect on the gluten matrix of large wheat 385
bran particles could be attributed to the breakage of secondary 386
structure of gluten macropolymer during dough kneading.⁴³ To 387
confirm this hypothesis, the dough system was investigated by 388
FT-IR. The secondary structures of gluten protein (Table 3) 389
are the α -helix, β -sheet, β -turn, random coil, and β -antiparallel. 390

Table 2. Calculation of the Porosity of Whole Wheat Bread Cross Section, Scanned by Magnetic Resonance Imaging, Processed Using the Threshold Segmentation Method^a

particle size (μm)	scanned layers	threshold value 1	N_1	threshold value 2	N_2	porosity ^b (%)
control (91.20)	1	30	134290	5	58218	37.74 \pm 5.25
	2	40	128756	5	64332	
	3	40	128096	5	48364	
50.21	1	50	208517	10	37163	33.35 \pm 9.32
	2	40	217024	10	56776	
	3	40	211807	10	36215	
96.99	1	50	123669	5	88162	38.21 \pm 9.22
	2	50	136608	5	60010	
	3	50	125912	5	94685	
235.40	1	80	154704	80	43971	29.96 \pm 5.08
	2	70	149476	50	39200	
	3	80	148623	80	32288	

^aThe pixels of twice threshold segmentation are represented by N_1 and N_2 . Each bread sample was scanned for three layers. ^bData are the mean value \pm standard deviation.

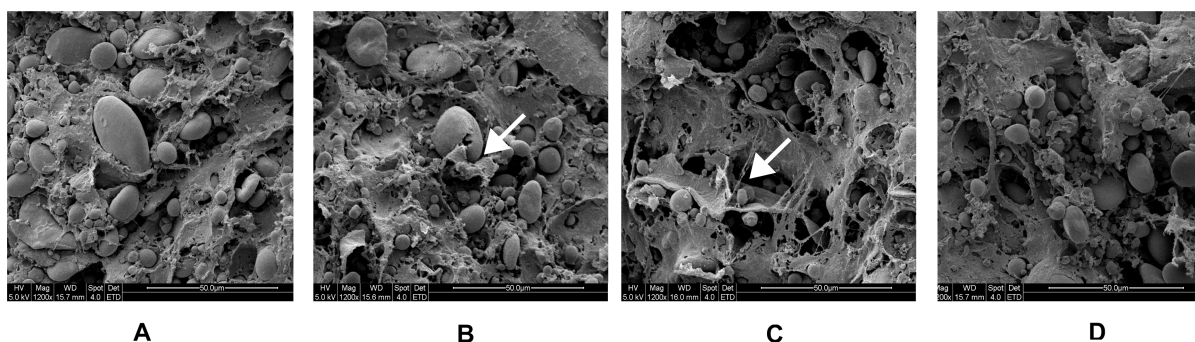


Figure 3. SEM images of whole wheat dough prepared with flour particle sizes of 50.21 μm (A), 96.99 μm (B), 235.40 μm (C), and 91.20 μm (control) (D), respectively. The arrows point to the wheat bran particles.

Table 3. Content of Secondary Structure (α -Helix, β -Sheet, β -Turn, Random Coil, and β -Antiparallel)^a of Gluten Protein in Whole Wheat Dough Prepared with Flour of Different Particle Sizes

flour particle size:	peak frequency (cm^{-1})			percentage ^b (%)		
	50.21 μm	96.99 μm	235.40 μm	50.21 μm	96.99 μm	235.40 μm
α -helix	1655.8	1656.7	1657	26.74 \pm 2.75	26.60 \pm 2.03	24.08 \pm 1.21
β -sheet	1617.2/1632	1617/1631.7	1617.1/1630.2	23.60 \pm 2.66	23.18 \pm 1.92	21.32 \pm 1.07
β -turn	1668.9	1669.5	1668.2	19.21 \pm 1.37	18.70 \pm 1.46	17.19 \pm 0.86
random coil	1644.5	1644.7	1648.6	20.10 \pm 1.40	21.41 \pm 2.05	28.14 \pm 1.15
β -antiparallel	1681.5	1682	1681	10.35 \pm 0.79	10.11 \pm 0.89	9.27 \pm 0.54

^aThe content of secondary structure of gluten protein was determined by FT-IR, represented by the percentage of peak area calculated from the fitted infrared spectrum. ^bMean \pm standard deviation (three replications).

Table 4. Content of Ferulic Acid Determined by RP-HPLC in Whole Wheat Flour of Different Particle Sizes

	particle size ^a			standard sample
	50.21 μm	96.99 μm	235.40 μm	
peak area	6691.6 \pm 6.4	2870.0 \pm 5.7	1816.7 \pm 4.4	7293.8 \pm 0.5
FA content (mg/mL)	0.9200 \pm 0.0010	0.3900 \pm 0.0008	0.2500 \pm 0.0006	1.00

^aMean \pm standard deviation (three replications).

391 The content of α -helix, β -sheet, β -turn, and β -antiparallel
392 increased with the refinement of bran (reduction in particle
393 size) contained in the WWF, while the content of random coil
394 showed the opposite trend. Textural properties of gluten
395 protein are mainly determined by the amount and balance of

weak and strong physical linkages, hydrogen bond, hydro- 396
phobic interactions, electrostatic forces, covalent bonds, and 397
disulfide bonds in dough system.⁴⁴ The secondary structures of 398
gluten protein play an important role in forming the gluten 399
network structure. Hydrogen bonds can be broken easily by 400

Table 5. T_2 Relaxation Time Distribution of Whole Wheat Dough of Different Flour Particle Sizes

	particle size								
	50.21 μm			96.99 μm			235.40 μm		
	T_{21}	T_{22}	T_{23}	T_{21}	T_{22}	T_{23}	T_{21}	T_{22}	T_{23}
percentage	0.0891	0.9042	0.0071	0.0563	0.9180	0.0123	/ ^a	0.9880	0.0122
SD ^b	0.0011	0.0020	0.0005	0.0008	0.0020	0.0008	/	0.0030	0.0007

^a/ indicates that no signal was detected. ^bSD, standard deviation.

Table 6. T_2 Relaxation Time Distribution of Whole Wheat Dough with Added Wheat Bran

	bran addition											
	control ^a			20%			40%			60%		
	T_{21}	T_{22}	T_{23}	T_{21}	T_{22}	T_{23}	T_{21}	T_{22}	T_{23}	T_{21}	T_{22}	T_{23}
% ^b	/ ^c	0.9981	0.0020	/	0.9892	0.0111	0.0274	0.9590	0.0143	0.0293	0.9571	0.0142
SD ^d		0.0028	0.0001		0.0030	0.0002	0.0001	0.0022	0.0001	0.0006	0.0025	0.0001

^aThe control groups were made with commercial white flour. ^bPercentage of each peak area in total areas (T_{21} , T_{22} , and T_{23}). ^c/ indicates that no signal was detected. ^dSD, standard deviation.

401 wheat bran during kneading,¹⁹ so the orderly secondary
402 structures of proteins can be split into disordered structures
403 like random coils. The higher content of α -helix, β -sheet, β -turn
404 and β -antiparallel structures in the refined particle size of
405 WWD, compared to the coarse group, suggested the
406 conformation of gluten structure of refined particle size was
407 more stable.⁴⁵ These results indicate that the large particle size
408 of WWF, especially the wheat bran with hard texture, had more
409 severe shearing effect on gluten proteins.

410 **Effect of WWF Granulation on the Content of Ferulic**
411 **Acid.** To investigate the mechanism through which WWF of
412 refined particle sizes had a destructive effect on the volume of
413 bread, the content of FA (Table 4) was determined by RP-
414 HPLC. Results showed that with the decreasing particle size of
415 WWF, more FA was released from the wheat bran to
416 participate in oxidative gelation. This can be attributed to the
417 disruption of cells and the increased specific surface area of
418 wheat bran.³⁷ Considering this theory, we confirmed that the
419 strength of AX gels would increase with reducing particle size of
420 WWF. This observation confirmed the hypothesis of
421 competitive water sequestration between the AX gels and the
422 gluten network, which verified that the bread made with refined
423 particle size WWF had less porosity.

424 **Demonstration of Water Migration between AX Gels**
425 **and Gluten by T_2 Relaxation Time.** To confirm that water
426 migration and competitive water sequestration between the AX
427 gels and gluten matrix were the primary causes for the inferior
428 baking quality of WWF, the T_2 relaxation times of WWD with
429 different particle size flours (Table 5) and wheat bran additions
430 (Table 6) were examined by MRI.

431 The T_2 relaxation time graph includes three peaks: T_{21} (0–1
432 ms), T_{22} (1–100 ms), and T_{23} (100–1000 ms), which
433 represent bound water, immobilized water, and free water,
434 respectively. The X-axis of the T_2 relaxation time represents the
435 water activity in the food system. A longer T_2 relaxation time
436 indicates a higher degree of water freedom. The Y-axis in the T_2
437 graph represents the signal amplitude of protons. The peak area
438 of T_2 represents the relative content of hydrogen protons and
439 the water absorption by hydrophilic components. The data
440 (Table 5) show that the proportion of T_{21} peak area percentage
441 had a negative correlation ($r = -0.991$) with the decrease in
442 particle size of the WWF. A positive correlation ($r = 0.996$) was
443 found between the proportion of T_{22} peak area percentage and

the average particle size of WWF. There was no change in the
444 peak area proportion of T_{23} . On the basis of the measurement
445 of T_2 relaxation time from MRI, we inferred that the T_{21} peak
446 area may represent the amount of water bound by the esterified
447 AX, essentially the cell wall material. The AX gels sequester
448 water and make it unavailable to migrate freely,⁴⁶ but there is
449 no effect on water activity (free water). These results implied
450 that the content of FA that participated in an oxidative gelation
451 reaction increased with the decrease in particle size of the
452 WWF. The AX gel strength was reported to have a positive
453 correlation with the content of FA;³⁵ therefore, as the particle
454 size of the WWF decreases, the AX gels will be strengthened
455 because of increased unesterified FA. In addition, AX gels
456 contain many hydrophilic groups such as hydroxyl groups,
457 which bond with water molecules through hydrogen bonds.⁴⁷
458 Although the porous structure of the gluten network also had
459 strong water absorption ability,⁴⁸ the water retention ability of
460 the gluten network is weaker than that of the AX gels, and the
461 AX has much greater water-holding capacity than gluten
462 proteins;⁴⁹ therefore, water tends to move from the gluten
463 matrix to AX gels. It was hypothesized that the AX gels
464 sequestered water, limiting the amount of water available to
465 participate in gluten formation in the bread dough,⁵⁰ and the
466 amount of AX gel influenced dough stickiness and water
467 retention capacity.⁵¹ 468

T_{22} may represent the water trapped in the gluten network
469 (immobilized water), which was the major existing form of
470 water. T_{23} may represent the free water distributed in the matrix
471 between the AX gels and the gluten network in the WWD
472 system. The amount of free water remained constant during the
473 entire water migration process between the AX gels and the
474 gluten network, which indicated that the amount of water lost
475 from the gluten network was similar to the amount of the water
476 obtained by the AX gels. This observation was in agreement
477 with the fact that the AX gels only sequester water and do not
478 affect water activity. This form of free water may be thought of
479 as “water migration channels” between the AX gels and the
480 gluten matrix. 481

The water sequestration competition mechanism between
482 the AX gels and the gluten matrix, as well as the identification
483 of each peak in the T_2 relaxation time experiment, was
484 confirmed by the study of wheat bran addition (Table 6). The
485 proportion of T_{21} peak area percentage had a positive 486

487 correlation ($r = 0.888$) with the increase in wheat bran addition
488 in white flour dough (Table 6); a negative correlation ($r =$
489 -0.893) was shown in the proportion of T_{22} peak area
490 percentage. However, T_{22} and T_{23} had strong signals in dough
491 systems that contained additional wheat bran. In the control
492 group and the dough with 20% wheat bran added, no T_{21} peak
493 was detected due to its weak signal. When the addition of wheat
494 bran was increased to 40%, T_{21} signals were detected.

495 In conclusion, the water migration from the gluten network
496 to AX gels as determined by the MRI technique confirmed that
497 it was the main cause leading to the inferior baking quality of
498 whole grain bread made with the refined particle size WWF.

499 ■ AUTHOR INFORMATION

500 Corresponding Author

501 *(G.G.H.) E-mail: ghou@wmcinc.org. Phone: +1 (503) 295-
502 0823. Fax: +1 (503) 295-2735. (Z.X.C.) E-mail: zxchen2007@
503 126.com. Phone: +86 510-8587911. Fax: +86 510-85867273.

504 Notes

505 The authors declare no competing financial interest.

506 ■ ACKNOWLEDGMENTS

507 We acknowledge Jin Lenong Agriculture Development Co.,
508 Ltd. (Henan Province, China), for providing the wheat sample
509 and technical assistance by the Shanghai Niumag Electronics
510 Technology Co., Ltd. (Shanghai, China).

511 ■ ABBREVIATIONS USED

512 AX, arabinoxylan; WWB, whole wheat bread; WWD, whole
513 wheat dough; WWF, whole wheat flour; MRI, magnetic
514 resonance imaging; FA, ferulic acid; AU, absorbance units;
515 RP-HPLC, reversed-phase high-performance liquid chromatog-
516 raphy; SEM, scanning electron microscope; FT-IR, Fourier
517 transform infrared spectroscopy.

518 ■ REFERENCES

- 519 (1) Rosell, C. M.; Victor, R. P.; Ronald Ross, W.; Vinood, B. P. The
520 science of doughs and bread quality. In *Flour and Breads and their*
521 *Fortification in Health and Disease Prevention*; Academic Press: San
522 Diego, CA, 2011; pp 3–14.
- 523 (2) Liu, R. H.; Okarter, N. Health benefits of whole grain
524 phytochemicals. *Crit. Rev. Food Sci. Nutr.* **2010**, *50*, 193–208.
- 525 (3) Vitaglione, P.; Napolitano, A.; Fogliano, V. Cereal dietary fibre: a
526 natural functional ingredient to deliver phenolic compounds into the
527 gut. *Trends Food Sci Technol.* **2008**, *19*, 451–463.
- 528 (4) Schatzkin, A.; Park, Y.; Leitzmann, M. F.; Hollenbeck, A. R.;
529 Cross, A. J. Prospective study of dietary fiber, whole grain foods, and
530 small intestinal cancer. *Gastroenterology* **2008**, *135*, 1163–1167.
- 531 (5) Liu, R. H. Whole grain phytochemicals and health. *J. Cereal Sci.*
532 **2007**, *46*, 207–219.
- 533 (6) Gelinias, P.; McKinnon, C. A finer screening of wheat cultivars
534 based on comparison of the baking potential of whole-grain flour and
535 white flour. *Int. J. Food Sci. Technol.* **2011**, *46*, 1137–1148.
- 536 (7) Jacobs, M. S.; Izydorczyk, M. S.; Preston, K. R.; Dexter, J. E.
537 Evaluation of baking procedures for incorporation of barley roller
538 milling fractions containing high levels of dietary fibre into bread. *J. Sci.*
539 *Food Agric.* **2008**, *88*, 558–568.
- 540 (8) Yu, L.; Slavin, M. All natural whole-wheat functional foods for
541 health promotion and disease prevention. In *Functional Food and*
542 *Health. ACS Symp. Series* **2008**, No. 993, 125–142.
- 543 (9) Moore, Z. Wheat bran particle size effects on bread baking
544 performance and quality. *J. Sci. Food Agric.* **1999**, *79*, 805–809.
- 545 (10) Salmenkallio-Marttila, M.; Katina, K.; Autio, K. Effects of bran
546 fermentation on quality and microstructure of high-fiber wheat bread.
547 *Cereal Chem.* **2001**, *78*, 429–435.

- (11) Gan, Z.; Ellis, P. R.; Vaughan, J. G.; Galliard, T. Some effects of 548
non-endosperm components of wheat and of added gluten on 549
wholemeal bread microstructure. *J. Cereal Sci.* **1989**, *10*, 81–91. 550
- (12) Moore, J. S. Shape-persistent molecular architectures of 551
nanoscale dimension. *Acc. Chem. Res.* **1997**, *30*, 402–413. 552
- (13) Gan, Z.; Galliard, T.; Ellis, P. R.; Angold, R. E.; Vaughan, J. G. 553
Effect of the outer bran layers on the loaf volume of wheat bread. *J.* 554
Cereal Sci. **1992**, *15*, 151–163. 555
- (14) Moder, K. F.; Bruinsma, B. L.; Ponte, J. G. Bread-making 556
potential of straight-grade and whole-wheat flours of Triumph and 557
Eagle-Plainsman V hard red winter wheats. *Cereal Chem.* **1984**, *61*, 558
269–273. 559
- (15) Piber, M.; Koehler, P. Identification of dehydroferulic acid- 560
tyrosine in rye and wheat: evidence for a covalent cross-link between 561
arabinoxylans and proteins. *J. Agric. Food Chem.* **2005**, *53*, 5276–5284. 562
- (16) Fausch, H.; Kundig, W.; Neukom, H. Ferulic acid as a 563
component of a glycoprotein from wheat flour. *Nature* **1963**, *199*, 564
287–287. 565
- (17) Markwalder, H. U.; Neukom, H. Diferulic acid as a possible 566
crosslink in hemicelluloses from wheat germ. *Phytochemistry* **1976**, *15*, 567
836–837. 568
- (18) Wang, M. W.; Hamer, R. J.; Van Vliet, T.; Oudgenoeg, G. 569
Interaction of water extractable pentosans with gluten protein: effect 570
on dough properties and gluten quality. *J. Cereal Sci.* **2002**, *36*, 25–37. 571
- (19) Autio, K. Effects of cell wall components on the functionality of 572
wheat gluten. *Biotechnol. Adv.* **2006**, *24*, 633–635. 573
- (20) Labat, E.; Rouau, X.; Morel, M. H. Effect of flour water- 574
extractable pentosans on molecular associations in gluten during 575
mixing. *Lebensm.-Wiss. -Technol. (Food Sci. Technol.)* **2002**, *35*, 185– 576
189. 577
- (21) Gill, S.; Vasanthan, T.; Ooraikul, B.; Rosnagel, B. Wheat bread 578
quality as influenced by the substitution of waxy and regular barley 579
flours in their native and extruded forms. *J. Cereal Sci.* **2002**, *36*, 219– 580
237. 581
- (22) Roman-Gutierrez, A. D.; Guilbert, S.; Cuq, B. Distribution of 582
water between wheat flour components: a dynamic water vapour 583
adsorption study. *J. Cereal Sci.* **2002**, *36*, 347–355. 584
- (23) Stapley, A. G. F.; Hyde, T. M.; Gladden, L. F.; Fryer, P. J. NMR 585
imaging of the wheat grain cooking process. *Int. J. Food Sci. Technol.* 586
1997, *32*, 355–375. 587
- (24) Hwang, S. S.; Cheng, Y. C.; Chang, C.; Lur, H. S.; Lin, T. T. 588
Magnetic resonance imaging and analyses of tempering processes in 589
rice kernels. *J. Cereal Sci.* **2009**, *50*, 36–42. 590
- (25) Horigane, A. K.; Takahashi, H.; Maruyama, S.; Ohtsubo, K. i.; 591
Yoshida, M. Water penetration into rice grains during soaking 592
observed by gradient echo magnetic resonance imaging. *J. Cereal Sci.* 593
2006, *44*, 307–316. 594
- (26) Ghosh, P. K.; Jayas, D. S.; Gruwel, M. L. H.; White, N. D. G. A 595
magnetic resonance imaging study of wheat drying kinetics. *Biosyst.* 596
Eng. **2007**, *97*, 189–199. 597
- (27) Shigehiro, N. I.; Hiroyuki, T.; Mika, K.; Hiromi, K. Routine 598
evaluation of the grain structures of baked breads by MRI. *Food Sci.* 599
Technol. Res. **2003**, *9*, 155–161. 600
- (28) Sapirstein, H. D.; Roller, R.; Bushuk, W. Instrumental 601
measurement of bread crumb grain by digital image analysis. *Cereal* 602
Chem. **1994**, *71*, 383–391. 603
- (29) Takano, H.; Ishida, N.; Koizumi, M.; Kano, H. Imaging of the 604
fermentation process of bread dough and the grain structure of baked 605
breads by magnetic resonance imaging. *J. Food Sci.* **2002**, *67*, 244–250. 606
- (30) Naito, S.; Ishida, N.; Takano, H.; Koizumi, M.; Kano, H. 607
Routine evaluation of the grain structures of baked breads by MRI. 608
Food Sci. Technol. Res. **2003**, *9*, 155–161. 609
- (31) Lodi, A.; Abduljalil, A. M.; Vodovotz, Y. Characterization of 610
water distribution in bread during storage using magnetic resonance 611
imaging. *Magn. Reson. Imaging* **2007**, *25*, 1449–1458. 612
- (32) Ishida, N.; Takano, H.; Naito, S.; Isobe, S.; Uemura, K.; Haishi, 613
T.; Kosse, K.; Koizumi, M.; Kano, H. Architecture of baked breads 614
depicted by a magnetic resonance imaging. *Magn. Reson. Imaging* **2001**, 615
19, 867–874. 616

- 617 (33) Brescia, M. A.; Sacco, D.; Sgaramella, A.; Pasqualone, A.;
618 Simeone, R.; Peri, G.; Sacco, A. Characterisation of different typical
619 Italian breads by means of traditional, spectroscopic and image
620 analyses. *Food Chem.* **2007**, *104*, 429–438.
- 621 (34) Wellner, N.; Mills, C.; Brownsey, G.; Wilson, R. H.; Brown, N.;
622 Freeman, J.; Halford, N. G.; Shewry, P. R.; Belton, P. S. Changes in
623 protein secondary structure during gluten deformation studied by
624 dynamic Fourier transform infrared spectroscopy. *Biomacromolecules*
625 **2005**, *6*, 255–261.
- 626 (35) Wang, M. W.; Oudgenoeg, G.; van Vliet, T.; Hamer, R. J.
627 Interaction of water unextractable solids with gluten protein: effect on
628 dough properties and gluten quality. *J. Cereal Sci.* **2003**, *38*, 95–104.
- 629 (36) Teukolsky, S. A.; Vetterling, W. T.; Flannery, B. P. Modeling of
630 data. In *Numerical Recipes in C: The Art of Scientific Computing*, 2nd ed.;
631 Cambridge University Press: New York, 1992; Vol. 2, pp 656–706.
- 632 (37) Noort, M. W. J.; van Haaster, D.; Hemery, Y.; Schols, H. A.;
633 Hamer, R. J. The effect of particle size of wheat bran fractions on bread
634 quality – evidence for fibre-protein interactions. *J Cereal Sci.* **2010**, *52*,
635 59–64.
- 636 (38) Cura, D. E.; Lantto, R.; Lille, M.; Andberg, M.; Kruus, K.;
637 Buchert, J. Laccase-aided protein modification: effects on the structural
638 properties of acidified sodium caseinate gels. *Int. Dairy J.* **2009**, *19*,
639 737–745.
- 640 (39) Stojceska, V.; Ainsworth, P. The effect of different enzymes on
641 the quality of high-fibre enriched brewer's spent grain breads. *Food*
642 *Chem.* **2008**, *110*, 865–872.
- 643 (40) Gan, Z.; Angold, R. E.; Williams, M. R.; Ellis, P. R.; Vaughan, J.
644 G.; Galliard, T. The microstructure and gas retention of bread dough.
645 *J. Cereal Sci.* **1990**, *12*, 15–24.
- 646 (41) Salmenkallio-Marttila, M.; Autio, K. Light microscopic
647 investigations of cereal grains, doughs and breads. *Lebensm.-Wiss.*
648 *-Technol. (Food Sci. Technol.)* **2001**, *34*, 18–22.
- 649 (42) Campbell, G. M.; Herrero-Sanchez, R.; Payo-Rodriguez, R.;
650 Merchan, M. L. Measurement of dynamic dough density and effect of
651 surfactants and flour type on aeration during mixing and gas retention
652 during proofing. *Cereal Chem.* **2001**, *78*, 272–277.
- 653 (43) Seyer, M.-E.; Gélinas, P. Bran characteristics and wheat
654 performance in whole wheat bread. *Int. J. Food Sci. Technol.*; **2009**,
655 *44*, 688–693.
- 656 (44) Selinheimo, E.; Autio, K.; Krijus, K.; Buchert, J. Elucidating the
657 mechanism of laccase and tyrosinase in wheat bread making. *J. Agric.*
658 *Food Chem.* **2007**, *55*, 6357–6365.
- 659 (45) Shewry, P. R.; Popineau, Y.; Lafiandra, D.; Belton, P. Wheat
660 glutenin subunits and dough elasticity: findings of the EUROWHEAT
661 project. *Trends Food Sci. Technol.* **2001**, *11*, 433–441.
- 662 (46) Elizabeth, C. M. Arabinoxylan gels: impact of the feruloylation
663 degree on their structure and properties. *Biomacromolecules* **2005**, *6*,
664 309–317.
- 665 (47) Izydorczyk, M. S.; Biliaderis, C. G. Cereal arabinoxylans:
666 advances in structure and physicochemical properties. *Carbohydr.*
667 *Polym.* **1995**, *28*, 33–48.
- 668 (48) Izydorczyk, M. S.; Chornick, T. L.; Paultey, F. G.; Edwards, N.
669 M.; Dexter, J. E. Physicochemical properties of hull-less barley fibre-
670 rich fractions varying in particle size and their potential as functional
671 ingredients in two-layer flat bread. *Food Chem.* **2008**, *108*, 561–570.
- 672 (49) Kweon, M.; Slade, L.; Levine, H. Solvent retention capacity
673 (SRC) testing of wheat flour: principles and value in predicting flour
674 functionality in different wheat-based food processes and in wheat
675 breeding—a review. *Cereal Chem.* **2011**, *88*, 537–552.
- 676 (50) Day, L.; Augustin, M. A.; Batey, I. L.; Wrigley, C. W. Wheat-
677 gluten uses and industry needs. *Trends Food Sci. Technol.* **2006**, *17*,
678 82–90.
- 679 (51) Bettge, A. D.; Morris, C. F. Oxidative gelation measurement and
680 influence on soft wheat batter viscosity and end-use quality. *Cereal*
681 *Chem.* **2007**, *84*, 237–242.